Biochemical and Biophysical Research Communications 572 (2021) 157–163

Contents lists available at ScienceDirect

Biochemical and Biophysical Research Communications

journal homepage: www.elsevier.com/locate/ybbrc

miRNAomics analysis reveals the promoting effects of cigarette smoke extract-treated Beas-2B-derived exosomes on macrophage polarization

Zhen Chen, Hao Wu, Rui Shi, Weiyang Fan, Jiashuo Zhang, Weiwei Su, Yonggang Wang, Peibo Li*

Guangdong Engineering and Technology Research Center for Quality and Efficacy Re-evaluation of Post-marketed TCM, State Key Laboratory of Biocontrol and Guangdong Provincial Key Laboratory of Plant Resources, School of Life Sciences, Sun Yat-sen University, Guangzhou, 510275, China

ARTICLE INFO

Article history:
Received 5 July 2021
Received in revised form
25 July 2021
Accepted 27 July 2021
Available online 5 August 2021

Keywords:
Cigarette smoke
Exosome
Macrophage polarization
miRNA
Airway epithelium

ABSTRACT

Inhalation of cigarette smoke induces airway and parenchyma inflammation that predisposes smokers to multiple lung diseases such as COPD. Macrophage polarization, an important specifying feature of inflammation, is involved in the progression of pulmonary inflammation. Exosomes and their loaded miRNAs provide a medium for cross-talk between alveolar macrophages and lung epithelial cells to maintain lung homeostasis. In this study, we treated Beas-2B with CSE to speculate the effects of Beas-2B-derived exosomes on macrophage polarization and performed exosomal miRNAomics analysis to explore the mechanism. We found that CSE-treated Beas-2B-derived exosomes could not only increase the percentages of $CD86^+$, $CD80^+$ $CD163^+$, and $CD206^+$ cells but also induce the secretion of TNF-α, IL-6, iNOS, IL-10, Arg-1, and TGF-β, indicating both M1 and M2 polarization of RAW264.7 macrophages were promoting. We performed miRNAomics analysis to identify 27 differentially expressed exosomal miRNAs such as miR-29a-3p and miR-1307-5p. Next, we obtained 14942 target genes of these miRNAs such as SCN1A and PLEKHA1 through the prediction of TargetScan and miRanda. We utilized KEGG enrichment analysis for these targets to identify potential pathways such as the PI3K-Akt signaling pathway and the MAPK signaling pathway on the regulation of macrophage polarization. We further found that miR-21-3p or miR-27b-3p may play critical roles in the promotion of CSE-Exo on macrophage polarization by miRNA interference. Collectively, this study provided novel information for diagnostic and therapeutic tactics of cigarette smoke-related lung diseases.

1. Introduction

The generated gas mixture from cigarette combustion contains approximately 4500 components, including carbon monoxide, nicotine, oxidants, fine particulate matter, and aldehydes [1]. Long-term exposure to cigarette smoke induces pulmonary inflammation, oxidative stress, and apoptosis, which predisposes to lead to chronic obstructive pulmonary disease (COPD), chronic bronchitis, emphysema, and lung cancer [2].

Alveolar macrophages (AMs) are the major immune cell population that removes cellular debris, particulate matter, and pathogens to regulate the local microenvironment and involve the inflammation progress in the lung [3]. Based on the environmental stimuli, macrophages can be classified into pro-inflammatory classically activated (M1) and anti-inflammatory alternatively activated (M2) phenotypes, which are antagonistic and reversible to each other [4]. Recent research shows that the cross-talk between AMs and lung epithelial cells (ECs) is essential to maintain lung homeostasis, which may help develop new therapeutic strategies for lung diseases [5].

Exosomes, extracellular vesicles ranging from 30 to 150 nm in diameter, contain proteins, lipids, metabolites, and nucleic acids and have been considered as a novel cell-cell communication mechanism [6]. Exosomal microRNAs (miRNAs)-mediated intercellular communication between many types of cells in the lung has been proved to affect biological pathways resulting in altered cellular functions and the development of pulmonary pathological states [7]. However, the functions of exosomes mediated cross-talk

* Corresponding author.
E-mail address: lipeibo@mail.sysu.edu.cn (P. Li).

https://doi.org/10.1016/j.bbrc.2021.07.093
0006-291X/

between AMs and lung ECs in respiratory inflammation have not been fully clarified.

Consequently, considering the biological functions of exosomes, in this study, we speculated whether cigarette smoke extract (CSE)-treated Beas-2B-derived exosomes can regulate macrophage polarization and revealed the specific mechanism through miRNAomics analysis and miRNA interference. Our findings provided novel information about the effects of exosomal miRNAs released from lung epithelium cells on macrophage polarization, which may be used to develop biomarkers for the diagnosis and therapies of cigarette smoke-related lung diseases.

2. Materials and methods

2.1. Cell culture and treatment

BEAS-2B cells were grown in high glucose DMEM (HyClone, Logan, UT, USA) plus 10% fetal bovine serum (CellCook, Guangzhou, China) and 1% penicillin/streptomycin (Invitrogen, Carlsbad, CA, USA) at 37 °C and 5% CO_2. RAW264.7 macrophages were grown in RPMI 1640 medium plus 10% fetal bovine serum and 1% penicillin/streptomycin at 37 °C and 5% CO_2. After being grown to 80–90% confluence, Beas-2B cells were switched to exosome-depleted DMEM (100,000×*g* overnight to remove the exosomes in fetal bovine serum).

Cigarette smoke extract (CSE) was prepared with a modification as previously reported [8]. The resultant CSE solution was regarded as 100% CSE and was diluted with medium to use in experiments within 1 h. For simplification, the abbreviations of each group of exosomes are as follows: Control-Exo: the Beas-2B cells were treated without any specific treatment, and supernatants were harvested after 24 h for exosome isolation; CSE-Exo: the Beas-2B cells were treated with 7.5% CSE for 24h and then isolated exosomes.

2.2. MTS assay

Beas-2B was seeded at 2×10^4 cells/cm^2 into 96-well plates and incubated for 12 h to allow the cells to attach. To test the effect of the CSE solution on cell viability, the cells in the blank control group were without any specifical treatment, while in the experimental groups were respectively treated with CSE at final concentrations of 2.5%, 5%, 7.5%, 10%, 12.5%, and 15%. After treating for 24 h, MTS solution (Promega, Madison, WI, USA) was added and incubated for 1 h. Then, the absorbance at 490 nm was recorded by an Epoch-2 microplate reader (BioTek, Winooski, VT, USA).

2.3. Exosome isolation

The supernatants of Beas-2B cells treated with or without CSE were harvested after 24 h to isolate exosomes. Briefly, the supernatants were centrifuged at 300×*g* for 10 min and 2000×*g* for 10 min to remove cells and dead cells. Then, the supernatants were centrifuged at 10,000×*g* for 30 min to eliminate cellular debris. Next, the supernatants were centrifuged in an L-100XP ultrafrigerated centrifuge (Beckman, Brea, CA, USA) at 100,000×*g* for 70 min to deposit exosome fractions. Finally, exosomes were resuspended with 200–300 μl PBS. All steps were performed at 4 °C. Exosomes were stored at −80 °C for subsequent use.

2.4. Identification of exosomes

Exosome imaging was performed utilizing transmission electronic microscopy (TEM, JEM-1400Flash, JEOL Ltd., Japan). To assess the size distribution of exosome particles, nanoparticle tracking analysis (NTA) was performed utilizing a NanoSight-NS300 (Malvern Instrument, Malvern, UK). The total protein concentration was determined using the bicinchoninic acid protocol (Beyotime, Nanjing, China) and the following western blotting analysis was performed to detect the marker proteins of exosomes. CD9 (1:2000, ab50249, Abcam, Cambridge, MA, USA), TSG101 (1:1000, ab125011, Abcam), ALIX (1:1000, ab275377, Abcam) were used in this procedure. The protein bands were detected by a chemiluminescence imaging system (Tanon, Shanghai, China).

2.5. Verification of exosome uptake

To determine whether RAW264.7 could uptake Beas-2B-derived exosomes, PKH67 green fluorescent (Sigma Aldrich, St. Louis, MO, USA) labeled exosomes according to the manufacturer's protocol. Labeled exosomes were incubated with RAW264.7 cells seeded on confocal dishes at 37 °C for 12 h. The nuclei of RAW264.7 macrophages were stained with 5 μg/ml 4′,6-diamidino-2-phenylindole (DAPI, Sigma). Images were acquired on an SP8X laser scanning confocal microscope (Leica, Wetzlar Germany).

2.6. Flow cytometry (FCM)

RAW264.7 macrophages were incubated in exosome-depleted RPMI 1640 and without any specifical treatment in the control group, while treated with 10 μg/ml Control-Exo and 3, 10, or 30 μg/ml CSE-Exo for 24 h in experiment groups. RAW264.7 macrophages in positive control groups for M1 and M2 polarization were treated with 500 ng/mL lipopolysaccharide (LPS) and 20 ng/mL interleukin (IL)-4, respectively, under the same condition. APC anti-mouse CD80, APC anti-mouse CD86, PE anti-mouse CD163, and PE anti-mouse CD206 (104713, 105113, 155307, 141705, Biolegend, Shenzhen, China) were used in this procedure. Then, the stained cells were analyzed by flow cytometry (CytoFLEX, Beckman).

2.7. Enzyme-linked immunosorbent assay (ELISA)

To further demonstrate the promoting effects of CSE-Exo on macrophage polarization, RAW264.7 macrophages were seeded at 5×10^4 cells/cm^2 into 6-well plates and treated with 10 μg/mL Control-Exo or CSE-Exo for 24 h. The concentrations of macrophage polarization-related cytokines in cell supernatants were determined using enzyme-linked immunosorbent assay (ELISA) assays (MeiMian, Wuhan, China) according to the manufacturer's instructions. The absorbance at 450 nm was recorded by a microplate reader.

2.8. Preparation of exosomal small RNA library and sequencing

Total RNA was extracted from the exosomes using an Exosome RNA Purification Kit (Norgen Biotek Corp, Thorold, Canada) according to the manufacturer's protocol. The total RNA quantity and purity were evaluated with a Bioanalyzer 2100 instrument (Agilent Technologies, Santa Clara, CA, USA). Approximately 500 ng of total RNA of samples was used to construct small RNA libraries through a TruSeq Small RNA Sample Prep Kit (Illumina, San Diego, CA, USA) according to the manufacturer's protocol. Further, the small RNA libraries were sequenced with single-end 50 bp sequencing on an Illumina Hiseq 2500 at the LC-BIO (Hangzhou, China).

2.9. Target gene prediction and functional enrichment analysis of differentially expressed exosomal miRNAs

Differentially expressed miRNAs based on normalized deep-sequencing counts were filtered using Student's t-test with the

significance threshold which was set to be 0.05. To predict the target genes of differentially expressed miRNAs, two computational target prediction algorithms (TargetScan and miRanda) were utilized at the LC-BIO cloud platform to identify the potential downstream targets. Predicted targets were filtered with TargetScan score >50 and miRanda binding energy < −10 and then mapped to obtain common targets. DAVID (http://david.abcc.ncifcrf.gov/) was used to perform Kyoto Encyclopedia of Genes and Genomes (KEGG) signaling pathway enrichment analysis for common targets.

To validate the miRNAomics, we performed real-time qPCR to validate the relative expression of 9 exosomal miRNAs which have been reported to be associated with the regulation of macrophage polarization. The real-time qPCR was carried out with GoTaq® qPCR Master Mix (Promega, Madison, WI, USA) on a LightCycler 480 (Roche, Mannheim, Germany). GADPH was used as endogenous controls for miRNA respectively. The relative expression of these miRNAs was calculated by the $2^{-\Delta CT}$ method and normalized to GADPH.

2.10. MicroRNA interference

To further explore which exosomal miRNAs played significant roles in promoting the polarization of macrophages in this study, miRNA interference was performed. RAW264.7 macrophages were seeded in six-well plates at 5×10^4 cells/plate on the day before the transfection. The cells were transfected with 100 pmol miRNA mimics, miRNA inhibitors, miRNA mimics negative control (NC), or miRNA inhibitors NC using Lipofectamine 3000 (Carlsbad, CA, USA) according to the manufacturer's protocol and cocultured with 10 μg/mL CSE-Exo for 24h. Then, we detected the polarization of RAW264.7 macrophages by FCM analysis of co-staining CD80 and CD163.

2.11. Statistical analysis

Statistical analyses were performed using one-way analysis of variance (ANOVA) or Student's t-test by GraphPad Prism 8 software. Statistical significance is indicated by p-values as follows: $p < 0.05$ (*) and $p < 0.01$ (**).

3. Results

3.1. Determined the optimal CSE concentration for Beas-2B

The effects of different concentrations of CSE solution on the viability of Beas-2B are shown in Fig. 1A. The results showed that CSE was non-toxic within the range of 2.5–7.5%, while significantly decreased cell viability at the range of 10–15%. In terms of the optimal tolerated CSE concentration for Beas-2B, we determined to perform subsequent studies at 7.5% CSE.

3.2. Identification of Beas-2B-derived exosomes

The TEM images showed that exosomes were cup or sphere-shaped with clear double-layered capsule morphology and the NTA showed that the average sizes of exosome particles were within 150 nm (Fig. 1B). Moreover, the western blotting showed that the bands of exosome marker proteins (ALIX, TSG101, and CD9) were clear (Fig. 1C). To sum up, it can be established that the ultrastructural vesicles isolated in this study are exosomes.

3.3. Verification of the exosomes uptake by RAW264.7 macrophages

We utilized the confocal microscope to observe whether macrophages could internalize Beas-2B-derived exosomes. The images

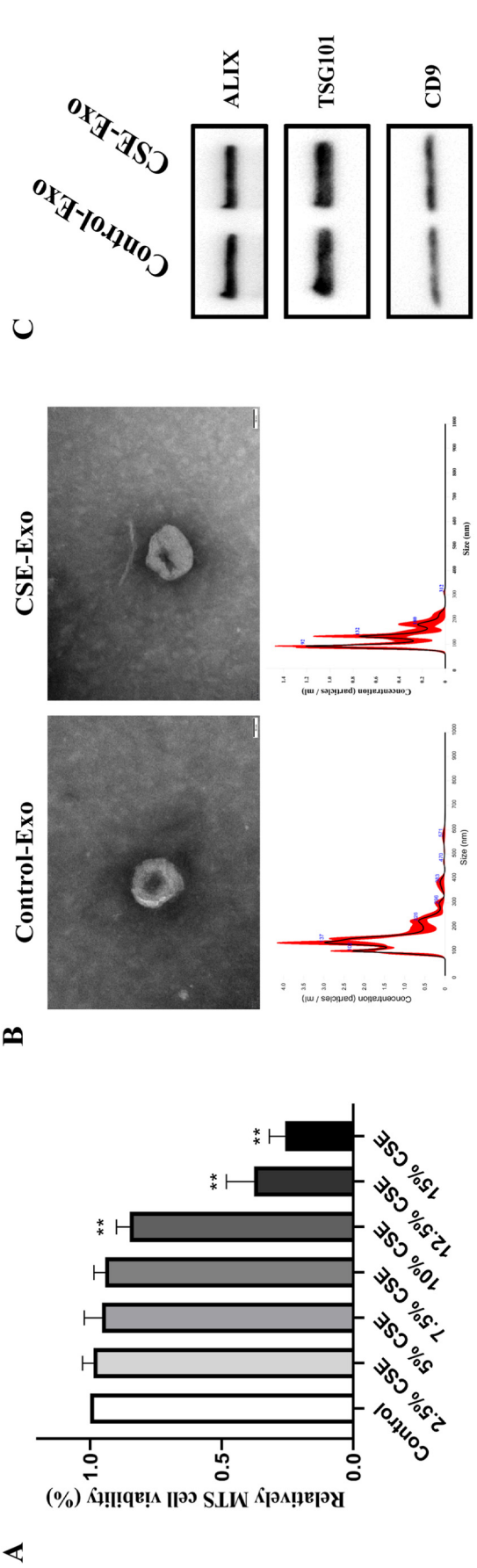

Fig. 1. (A) Effect of different concentrations of CSE solution on the viability of Beas-2B (n = 6). **P < 0.01 vs. control group. (B) Morphology of exosomes by transmission electron microscope (scale bars = 50 nm) and size distribution of exosomes performed by nanoparticle tracking analysis; (C) Western blotting for ALIX, TSG101, and CD9 in exosomes.

showed that the punctate green fluorescence exosomes were distributed around the nuclei of RAW264.7 macrophages stained by blue fluorescence, indicating that exosomes were efficiently taken up into the cytoplasm of macrophages (Fig. 2).

3.4. CSE-exo promoted both M1 and M2 polarization of RAW264.7 macrophages

We next performed FCM analysis to detect the effects of CSE-Exo on macrophage polarization. The results showed, compared with the Control-Exo group, the percentages of M1 macrophages (indicated by $CD86^+$ and $CD80^+$ cells) and M2 macrophages (indicated by $CD163^+$ and $CD206^+$ cells) were markedly increased with the treatment of CSE-Exo in a dose-effect manner, suggesting that CSE-Exo induced both M1 and M2 polarization of RAW264.7 macrophages (Fig. 3A).

3.5. CSE-exo induced the secretion of polarization-related cytokines of RAW264.7 macrophages

The effects of CSE-Exo on the release of macrophage polarization-related cytocines were determined using ELISA assays. The results showed, compared with the Control-Exo group, 10 μg/mL CSE-Exo could significantly induce the secretion of M1-related cytokines (TNF-α, IL-6, and iNOS) and M2-related cytokines (IL-10, Arg-1, and TGF-β) of RAW264.7 cells, further indicating the promoting effects of CSE-Exo on both M1 and M2 polarization of macrophage (Fig. 3B).

3.6. Target gene prediction and functional enrichment analysis of exosomal miRNAs

We next determined the miRNA composition in exosomes isolated from untreated or CSE-treated Beas-2B cells using next-generation sequencing. A total of 1139 miRNAs were identified and 27 miRNAs demonstrated significant changes ($p < 0.05$) in exosomes derived from CSE-treated Beas-2B cells compared to control. All significantly changed miRNAs are listed in Table S1, including 8 upregulated miRNAs such as miR-29a-3p and miR-1307-5p and 19 downregulated miRNAs such as miR-92a-3p and miR-106b-3p.

A total of 15257 and 17031 downstream targets of 27 differentially expressed exosomal miRNAs were predicted from TargetScan and miRanda, respectively. Predicted targets were mapped to obtain 14942 common targets and the top 20 targets ranking by TargetScan score and miRanda binding energy were shown in Table S2. The sodium channel protein type 1 subunit alpha (SCN1A) was the potential target with the highest score. Other high-scoring targets included the fragile X mental retardation syndrome-related protein 1 (FXR1), pleckstrin homology domain-containing family A member 1 (PLEKHA1), and so on. Then, we utilized the David to perform KEGG enrichment analysis for common targets and visualized the top 20 enriched signaling pathways ranking by gene count including the PI3K-Akt signaling pathway, the MAPK signaling pathway, the Ras signaling pathway, and so on in Fig. 4A.

3.7. miR-21-3p and mir-27b-3p played critical roles in the promotion of CSE-Exo on macrophage polarization

Among 27 significantly changed exosomal miRNAs, we screened 9 miRNAs that have been reported to be associated with the regulation of macrophage polarization through literature review, including miR-29a-3p, miR-21-3p, miR-27b-3p, miR-30b-5p, let-7d-5p, miR-425-5p, miR-25-3p, miR-145-5p, and miR-192-5p. The real-time qPCR results showed that the changing trend of 6 of these exosomal miRNAs was consistent with our miRNAomics (Fig. 4B). Then, the results of miRNA interference showed that the ratio of $CD80^+$ and $CD163^+$ macrophage were both significantly reduced compared with the CSE-Exo group after being transfected with miR-21-3p or miR-27b-3p inhibitor (Fig. 4C). These findings indicated that miR-21-3p and miR-27b-3p may be the critical exosomal miRNAs that promoted macrophage polarization.

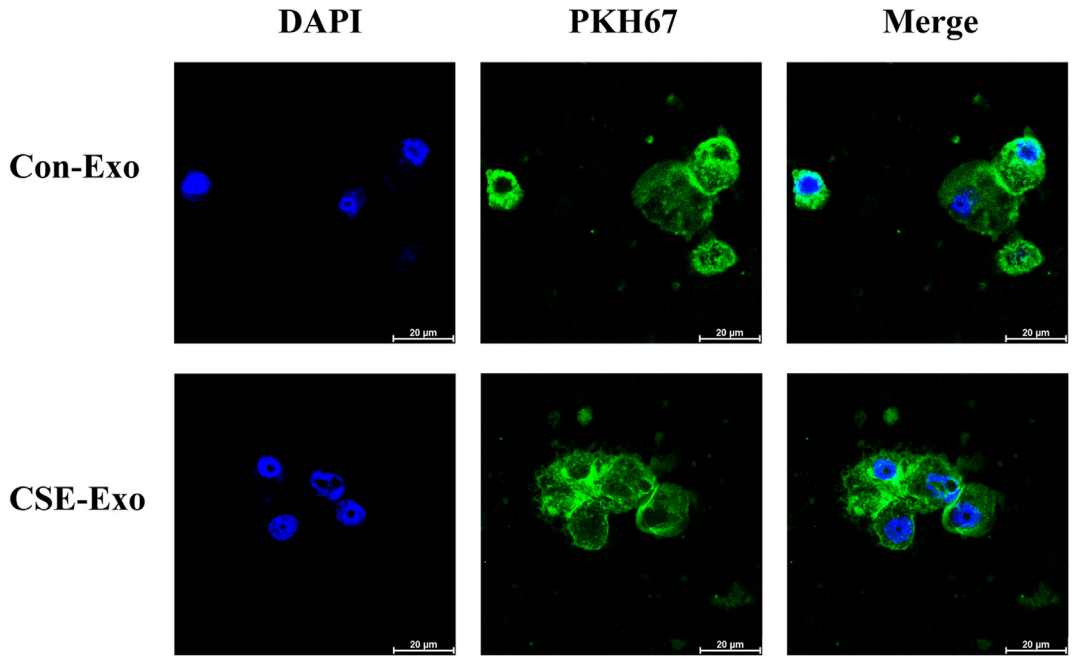

Fig. 2. The detection of internalized exosomes imaged by confocal microscopy (PKH67 in green, DAPI in blue, scale bars = 20 μm). (For interpretation of the references to color in this figure legend, the reader is referred to the Web version of this article.)

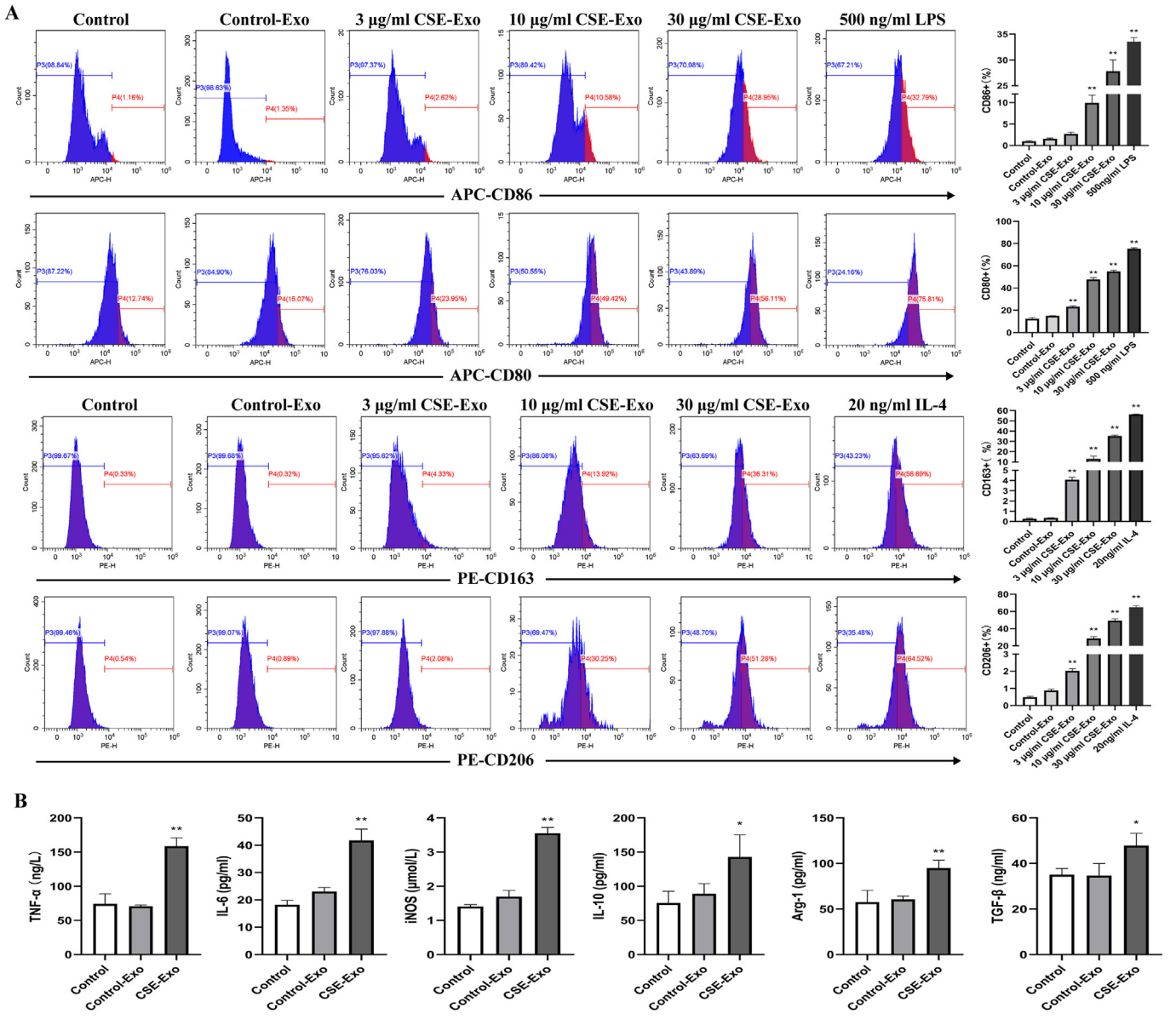

Fig. 3. CSE-Exo promoted RAW264.7 switching into both the M1 and M2 phenotype (A) The percentages of M1-polarized macrophages were analyzed by measuring $CD86^+$ or $CD80^+$ cells and the percentages of M2-polarized macrophages were analyzed by measuring $CD163^+$ or $CD206^+$ cells (n = 3); (B) The concentrations of M1-related cytocines (TNF-α, IL-6, and iNOS) and M2-related cytocines (IL-10, Arg-1, and TGF-β) (n = 3). *P < 0.05 vs. Control-Exo group. **P < 0.01 vs. Control-Exo group.

4. Discussions and conclusions

Cigarette smoke contains thousands of different compounds and many of these components are irritants, suspected carcinogens, and pro-inflammatory agents, which are considered to be major drivers of the onset and progression of lung disease. Under normal physiological status, lung ECs maintain AMs in a quiescent state to keep lung homeostasis. When pathogens invaded the epithelium or airway, the disruption of this homeostasis may lead to the activation of AMs and initiation of inflammation [9]. Exosomes have been proved to provide a medium for cellular cross-talk between AMs and ECs in the complex lung microenvironment [10]. Lee et al. [11] found that lung ECs-derived extracellular vesicles could activate pro-inflammatory functions of AMs, resulting in promoting the recruitment of immunomodulatory cells involved in lung injury.

In this study, we found that CSE-treated Beas-2B-derived exosomes significantly increased the percentages of $CD86^+$, $CD80^+$ $CD163^+$, and $CD206^+$ cells and induced the secretion of polarization-related cytokines of RAW264.7 macrophages, suggesting that both M1 and M2 phenotypes of macrophages were increased. Supporting this, Wang et al. [12] mentioned that exosomes derived from CSE-treated mouse airway epithelial cells promoted M1 macrophage polarization by upregulating triggering receptor expressed on myeloid cells-1 expression, thereby aggravating the development of COPD. However, He et al. [13] demonstrated that CSE-treated bronchial epithelia cells-derived extracellular vesicles relieved the epithelial-mesenchymal transition involved in COPD pathogenesis by alleviating M2 macrophage polarization, which was opposite to the regulation of M2 macrophage polarization in the present study. The extracellular vesicles were co-cultured with macrophages for 48 h in He's study, while 24 h in the present study. Probably due to the stress response of macrophages, M2 macrophages were significantly promoted in the short term to accelerate the vanish of inflammation. Support this

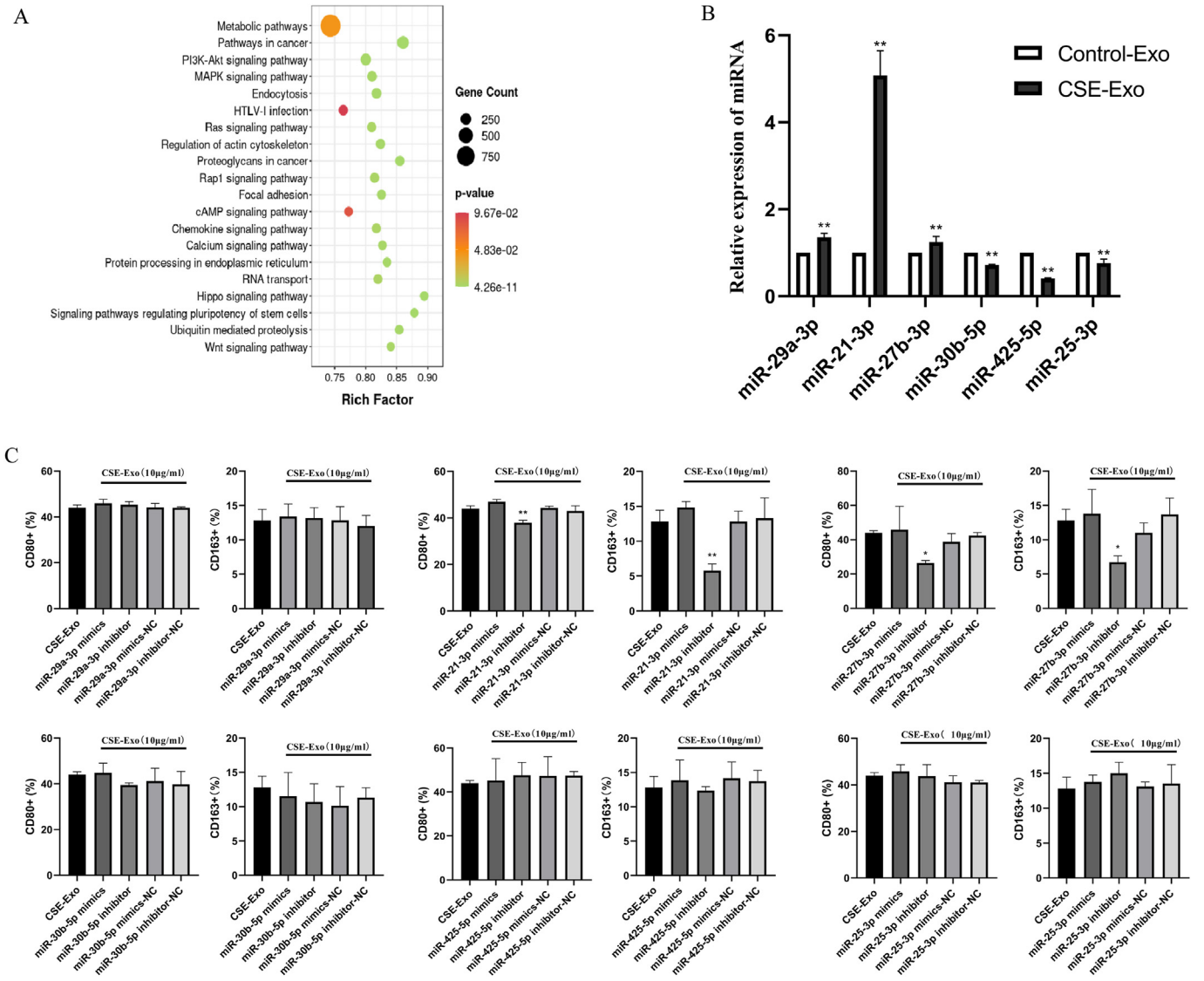

Fig. 4. (A) KEGG enrichment analysis for predicted common targets. The top 20 pathways ranking by gene count are shown. The size of the node represents the number of target genes in the pathway and the color of the dot reflects the p-value. (B) Relative expression of specific miRNAs in CSE-treated Beas-2B-derived exosomes and control exosomes (n = 5). **P < 0.01 vs. Control-Exo group. (C) The ratios of $CD80^+$ and $CD163^+$ cells of RAW264.7 macrophages were detected by flow cytometry (n = 3). *P < 0.05 vs. CSE-Exo group. **P < 0.01 vs. CSE-Exo group. (For interpretation of the references to color in this figure legend, the reader is referred to the Web version of this article.)

point, Feng et al. [14] found that rat alveolar and peritoneal macrophages towards M2 polarization at 9–24h of CSE exposure.

Present evidence has proved that extracellular vesicles miRNAs provide novel diagnostic biomarkers for multiple lung diseases and may be used for therapeutic interventions [15]. In the present study, we identified 27 significantly changed miRNAs in exosomes derived from CSE-treated Beas-2B cells compared to control, of which 9 miRNAs have been reported to be associated with the regulation of macrophage polarization. We further found that the downregulation of miR-21-3p or miR-27b-3p could reverse the promoting effects of CSE-Exo on macrophage polarization through miRNA interference. Supporting this, Yao et al. [16] proved that mesenchymal stem cells-derived exosomal miR-21 was abundantly upregulated upon IL-1β stimulation and transferred to macrophages, leading to M2 polarization thereby ameliorating sepsis. The therapeutic efficacy of these exosomes was partially lost upon inhibiting miR-21. Furthermore, Wang et al. [17] revealed that miR-27-3p regulated pro-inflammatory cytokine production and alveolar macrophage polarization depending on TLR2/4 intracellular signaling by targeting peroxisome proliferator-activated receptor γ in mice exposed to cigarette smoke/lipopolysaccharide. These two miRNAs may be the critical exosomal miRNAs that promoted macrophage polarization in our study but the downstream exact mechanisms need further investigation.

miRNAs are general-purpose specific factors in post-transcriptional gene silencing, so identifying their targets has become a key strategy to understand their roles in the development of disease [18]. In this study, among the top 20 target genes ranking by score values, 5 targets were reported to be involved in the regulation of macrophage polarization. Jaiswal et al. [19] identified that angiotensin-II induced Lin28B negatively regulates the mature process of miR-99a, which led to M2 macrophage inhibition and M1 macrophage promotion in ovalbumin-induced airway inflammation mice. Im et al. [20] found that the blocking antibody to FGF2 in combination with radiotherapy was found to reduce or even eliminate tumor regrowth in association with an increase in the

M1/M2 ratio of tumor-associated macrophages. Moreover, Sema3A, FXR1, and CBLB have been demonstrated to be correlated to the activation of macrophages [21–23]. These findings suggested that the above target genes including Lin28B, FGF2, Sema3A, FXR1, and CBLB may play key roles in regulating macrophage polarization in the present study.

Through KEGG enrichment analysis, we found multiple potential signaling pathways and available evidence has shown that various signaling cascade responses involve in the regulation of macrophage polarization. Lu et al. [24] found that M2 macrophage polarization was promoted in emphysematous mice, which was mediated through PI3K/Akt pathway activation. Significantly, tuberous sclerosis complex 1 and progranulin have been shown to inhibit M1 macrophage polarization respectively via Ras signaling pathway and MAPK signaling pathway thereby exerting anti-inflammatory effects [25,26]. Furthermore, cAMP signaling pathway, chemokine signaling pathway, Hippo signaling pathway, and Wnt signaling pathway also have been proved to regulate the progress of macrophage polarization involved in inflammation or tumor growth [27–30]. These signaling pathways need to be concerned in further studies.

In conclusion, we found that CSE-treated Beas-2B-derived exosomes promoted the polarization of RAW264.7 macrophages towards both M1 and M2 phenotypes. The miRNAomics analysis indicated potential miRNAs, target genes, and signaling pathways that were associated with macrophage polarization in the present study. The further miRNA interference suggested that miR-21-3p and miR-27b-3p may be the critical exosomal miRNAs that promoted macrophage polarization. Our study provided novel information for potential utilization as diagnostic biomarkers and identification of therapeutic targets of cigarette smoke-related lung diseases.

Declaration of competing interest

The authors declare that they have no known competing financial interests or personal relationships that could have appeared to influence the work reported in this paper.

Acknowledgment

This work was financially supported by the Applied Science and Technology R&D Special Fund Project of Guangdong Province (No. 2016B020239003) and the Science and Technology Program of Guangdong Province (No. 2019B090905002).

Appendix A. Supplementary data

Supplementary data to this article can be found online at https://doi.org/10.1016/j.bbrc.2021.07.093.

References

[1] W. Hou, S. Hu, C. Li, et al., Cigarette smoke-induced lung barrier dysfunction, EMT, and tissue remodeling: a possible link between COPD and lung cancer, Biomed. Res. Int. 2019 (2019) 2025636.
[2] A. Strzelak, A. Ratajczak, A. Adamiec, et al., Tobacco smoke induces and alters immune responses in the lung triggering inflammation, allergy, asthma and other lung diseases: a mechanistic review, Int. J. Environ. Res. Public Health 15 (5) (2018) 1033.
[3] P. Cheng, S. Li, H. Chen, Macrophages in lung injury, repair, and fibrosis, Cells-Basel 10 (2) (2021) 436.
[4] Y. Kim, S. Nurakhayev, A. Nurkesh, et al., Macrophage polarization in cardiac tissue repair following myocardial infarction, Int. J. Mol. Sci. 22 (5) (2021) 2715.
[5] E.Y. Bissonnette, J.F. Lauzon-Joset, J.S. Debley, et al., Cross-talk between alveolar macrophages and lung epithelial cells is essential to maintain lung homeostasis, Front. Immunol. 11 (2020) 583042.
[6] M. Yamada, Extracellular vesicles: their emerging roles in the pathogenesis of respiratory diseases, Respir. Investig. 59 (3) (2021) 302–311.
[7] S.D. Alipoor, E. Mortaz, J. Garssen, et al., Exosomes and exosomal miRNA in respiratory diseases, Mediat. Inflamm. 2016 (2016) 5628404.
[8] P. Chen, Z. Xiao, H. Wu, et al., Beneficial effects of naringenin in cigarette smoke-induced damage to the lung based on bioinformatic prediction and in vitro analysis, Molecules 25 (20) (2020) 4704.
[9] L. Guillot, N. Nathan, O. Tabary, et al., Alveolar epithelial cells: master regulators of lung homeostasis, Int. J. Biochem. Cell. Biol. 45 (11) (2013) 2568–2573.
[10] S. Bartel, J. Deshane, T. Wilkinson, et al., Extracellular vesicles as mediators of cellular cross-talk in the lung microenvironment, Front. Med. (Lausanne) 7 (2020) 326.
[11] H. Lee, D. Zhang, Z. Zhu, et al., Epithelial cell-derived microvesicles activate macrophages and promote inflammation via microvesicle-containing microRNAs, Sci. Rep. 6 (2016) 35250.
[12] L. Wang, Q. Chen, Q. Yu, et al., Cigarette smoke extract-treated airway epithelial cells-derived exosomes promote M1 macrophage polarization in chronic obstructive pulmonary disease, Int. Immunopharm. 96 (2021) 107700.
[13] S. He, D. Chen, M. Hu, et al., Bronchial epithelial cell extracellular vesicles ameliorate epithelial-mesenchymal transition in COPD pathogenesis by alleviating M2 macrophage polarization, Nanomedicine 18 (2019) 259–271.
[14] H. Feng, Y. Yin, Y. Ren, et al., Effect of CSE on M1/M2 polarization in alveolar and peritoneal macrophages at different concentrations and exposure in vitro, In Vitro Cell. Dev. Biol. Anim. 56 (2) (2020) 154–164.
[15] J. Chen, C. Hu, P. Pan, Extracellular vesicle microRNA transfer in lung diseases, Front. Physiol. 8 (2017) 1028.
[16] M. Yao, B. Cui, W. Zhang, et al., Exosomal miR-21 secreted by IL-1β-primed-mesenchymal stem cells induces macrophage M2 polarization and ameliorates sepsis, Life Sci. 264 (2021) 118658.
[17] D. Wang, S. He, B. Liu, et al., miR-27-3p regulates TLR2/4-dependent mouse alveolar macrophage activation by targetting PPARγ, Clin. Sci. (Lond.) 9 (132) (2018) 943–958.
[18] B. Liu, J. Li, M.J. Cairns, Identifying miRNAs, targets and functions, Brief Bioinform. 15 (1) (2014) 1–19.
[19] A. Jaiswal, M. Maurya, P. Maurya, et al., Lin28B regulates angiotensin II-mediated let-7c/miR-99a microRNA formation consequently affecting macrophage polarization and allergic inflammation, Inflammation 43 (5) (2020) 1846–1861.
[20] J.H. Im, J.N. Buzzelli, K. Jones, et al., FGF2 alters macrophage polarization, tumour immunity and growth and can be targeted during radiotherapy, Nat. Commun. 11 (1) (2020) 4064.
[21] M. Rienks, P. Carai, N. Bitsch, et al., Sema3A promotes the resolution of cardiac inflammation after myocardial infarction, Basic Res. Cardiol. 112 (4) (2017) 42.
[22] J. Garnon, C. Lachance, S. Di Marco, et al., Fragile X-related protein FXR1P regulates proinflammatory cytokine tumor necrosis factor expression at the post-transcriptional level, J. Biol. Chem. 280 (7) (2005) 5750–5763.
[23] T. Abe, K. Hirasaka, T. Nikawa, Involvement of Cbl-b-mediated macrophage inactivation in insulin resistance, World J. Diabetes 8 (3) (2017) 97–103.
[24] J. Lu, L. Xie, C. Liu, et al., PTEN/PI3k/AKT regulates macrophage polarization in emphysematous mice, Scand. J. Immunol. 85 (6) (2017) 395–405.
[25] L. Zhu, T. Yang, L. Li, et al., TSC1 controls macrophage polarization to prevent inflammatory disease, Nat. Commun. 5 (2014) 4696.
[26] L. Liu, H. Guo, A. Song, et al., Progranulin inhibits LPS-induced macrophage M1 polarization via NF-κB and MAPK pathways, BMC Immunol. 21 (1) (2020) 32.
[27] K. Yamamichi, T. Fukuda, T. Sanui, et al., Amelogenin induces M2 macrophage polarisation via PGE2/cAMP signalling pathway, Arch. Oral Biol. 83 (2017) 241–251.
[28] P. Ruytinx, P. Proost, J. Van Damme, et al., Chemokine-induced macrophage polarization in inflammatory conditions, Front. Immunol. 9 (2018) 1930.
[29] Q. Luo, J. Luo, Y. Wang, YAP deficiency attenuates pulmonary injury following mechanical ventilation through the regulation of M1/M2 macrophage polarization, J. Inflamm. Res. 13 (2020) 1279–1290.
[30] X. Tian, Y. Wu, Y. Yang, et al., Long noncoding RNA LINC00662 promotes M2 macrophage polarization and hepatocellular carcinoma progression via activating Wnt/β-catenin signaling, Mol. Oncol. 14 (2) (2020) 462–483.